JCI insight

RESEARCH ARTICLE

Natural single-nucleotide deletion in chymotrypsinogen C gene increases severity of secretagogue-induced pancreatitis in C57BL/6 mice

Andrea Geisz,[1] Zsanett Jancsó,[1] Balázs Csaba Németh,[1] Eszter Hegyi,[1] and Miklós Sahin-Tóth[1,2]

[1]Center for Exocrine Disorders, Department of Molecular and Cell Biology, Henry M. Goldman School of Dental Medicine, Boston University, Boston, Massachusetts, USA. [2]Department of Surgery, UCLA, Los Angeles, California, USA.

Genetic susceptibility to chronic pancreatitis in humans is frequently associated with mutations that increase activation of the digestive protease trypsin. Intrapancreatic trypsin activation is an early event in experimental acute pancreatitis in rodents, suggesting that trypsin is a key driver of pathology. In contrast with trypsin, the pancreatic protease chymotrypsin serves a protective function by mitigating trypsin activation through degradation. In humans, loss-of-function mutations in chymotrypsin C (CTRC) are common risk factors for chronic pancreatitis; however, the pathogenic effect of CTRC deficiency has not been corroborated in animal models yet. Here we report that C57BL/6 mice that are widely used for genetic manipulations do not express functional CTRC because of a single-nucleotide deletion in exon 2 of the *Ctrc* gene. We restored a functional *Ctrc* locus in C57BL/6N mice and demonstrated that in the *Ctrc*$^{+}$ strain, the severity of cerulein-induced experimental acute and chronic pancreatitis was significantly ameliorated. Improved disease parameters were associated with reduced intrapancreatic trypsin activation, suggesting a causal link between CTRC-mediated trypsinogen degradation and protection against pancreatitis. Taken together with prior human genetic and biochemical studies, the observations provide conclusive evidence for the protective role of CTRC against pancreatitis.

Introduction

The inflammatory disease continuum of the pancreas starts with a sentinel attack of acute pancreatitis, followed by recurrent acute pancreatitis attacks with eventual progression to chronic pancreatitis (1). The pathological drivers underlying the inflammatory process are frequently genetic mutations that promote the premature, intrapancreatic activation of the digestive protease trypsin (2). The high-impact susceptibility genes that influence activation of trypsinogen to trypsin include *PRSS1* (serine protease 1, cationic trypsinogen), *SPINK1* (serine protease inhibitor Kazal type 1) and *CTRC* (chymotrypsin C). Gain-of-function mutations in PRSS1 promote trypsinogen activation whereas loss-of-function mutations in SPINK1 and CTRC impair protective trypsin inhibition and trypsinogen degradation, respectively (2). CTRC is a minor chymotrypsin isoform capable of degrading trypsinogen and thereby suppressing its activation to trypsin (2–4). The clinically most common PRSS1 mutations cause hereditary pancreatitis by rendering trypsinogen resistant to protective degradation by CTRC and thereby increasing intrapancreatic trypsin activity (2, 4). Although the principal action of CTRC is to promote trypsinogen degradation, it also enhances trypsinogen activation by processing the cationic trypsinogen activation peptide to a shorter form, which is more sensitive to trypsin-mediated activation (4–6). This minor effect becomes important only when certain cationic trypsinogen mutations (e.g., p.A16V) hijack this mechanism and thereby stimulate trypsinogen activation to a pathological extent (4, 5, 7). A defensive role for chymotrypsin-mediated trypsinogen degradation was further corroborated by the recent observation that a commonly occurring 16.6-kb inversion at the human *CTRB1-CTRB2* locus (encoding chymotrypsin B1 and B2) has a small but significant effect on pancreatitis risk (8). The minor inversion allele alters the expression ratio of the 2 isoforms in such a manner that trypsinogen degradation becomes more efficient, resulting in a small protective effect against pancreatitis. Taken together, human genetic and biochemical evidence indicates that chymotrypsin-dependent trypsinogen control is essential for pancreas health and protection against pancreatitis.

Authorship note: AG and ZJ contributed equally to this work.

Conflict of interest: The authors have declared that no conflict of interest exists.

Submitted: April 22, 2019
Accepted: June 13, 2019
Published: July 25, 2019.

Reference information: *JCI Insight*. 2019;4(14):e129717. https://doi.org/10.1172/jci.insight.129717.

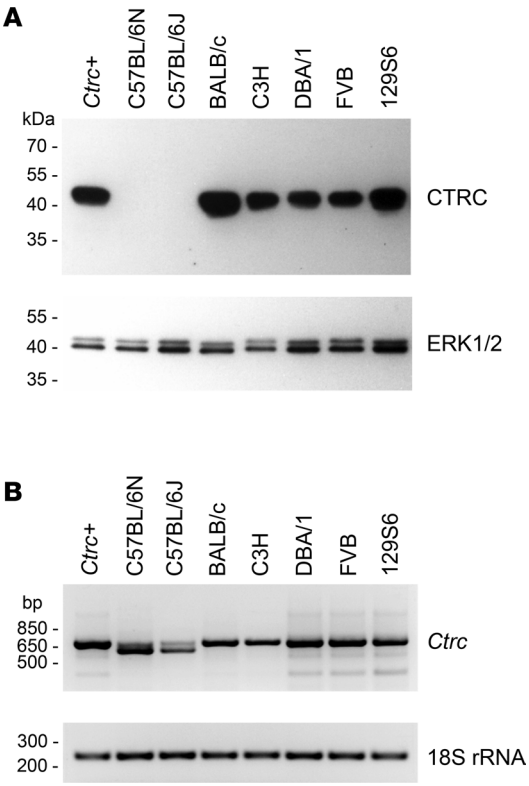

Figure 1. Expression of CTRC in the mouse pancreas. (**A**) Expression of CTRC protein in the pancreas of 7 inbred mouse strains and the *Ctrc*$^{+}$ strain. Pancreas homogenates (10 μg total protein) from the indicated mice were analyzed by Western blotting. ERK1/2 protein was measured as loading control. (**B**) Expression of *Ctrc* mRNA in the pancreas of 7 inbred mouse strains and the *Ctrc*$^{+}$ strain, determined by RT-PCR and agarose gel electrophoresis. 18S rRNA was measured as loading control. Representative gels from 2 independent experiments are shown.

To confirm the notion that loss of chymotrypsin function increases intrapancreatic trypsin activation and worsens pancreatitis, we recently generated a mouse strain deficient in CTRB1, the major chymotrypsin isoform in mice (9). Previously, using purified proteins, we demonstrated that mouse trypsinogens may be regulated by mouse CTRC and CTRB1 through degradation and regulatory cleavages that suppress activation (10). When given repeated injections of supramaximal stimulatory doses of cerulein, *Ctrb1-del* mice developed severer pancreatitis than C57BL/6N control mice. Importantly, intrapancreatic trypsin activation was significantly elevated in *Ctrb1-del* mice, confirming the protective role of chymotrypsin-dependent trypsinogen degradation (10). Although these findings were important conceptually, they did not address the specific role of CTRC, the chymotrypsin isoform more relevant to human disease. Therefore, in the present study we set out to characterize CTRC expression in different mouse strains with the intent of correlating experimental pancreatitis responses to pancreatic CTRC levels. Surprisingly, we found that the popular inbred C57BL/6 mice did not express functional CTRC because of a natural single-nucleotide deletion. We restored a functional *Ctrc* gene in C57BL/6N mice and studied experimental pancreatitis responses in the *Ctrc*$^{+}$ strain. The results presented below offer long-awaited animal model evidence for the predicted protective role of CTRC in pancreatitis.

Results

C57BL/6 mice are naturally deficient in CTRC. To investigate whether variations in CTRC expression affect pancreatitis severity, first we compared CTRC protein levels in the pancreas of 7 inbred mouse strains. Unexpectedly, we found that C57BL/6 mice, including both the N and J substrains, expressed no detectable CTRC protein, as judged by Western blotting of pancreas extracts. In contrast, all other mice tested contained comparable levels of pancreatic CTRC protein (Figure 1A). Consistent with the protein expression defect, reverse transcription PCR (RT-PCR) analysis of *Ctrc* mRNA in the pancreas of C57BL/6 mice yielded 2 abnormal products. DNA sequencing revealed that the faint larger band contained a single nucleotide deletion (c.117delT) and the more prominent smaller band a 98-nucleotide deletion corresponding to exon 3 (Figure 1B). As expected, RT-PCR amplicons from the pancreas of the other mouse strains showed the expected size and a DNA sequence with no deletion (Figure 1B). We confirmed the c.117delT deletion in exon 2 of the *Ctrc* gene on chromosome 4 in the National Center for Biotechnology Information genomic reference sequence NC_000070.6 (*Mus musculus* strain C57BL/6J chromosome 4, GRCm38.p4

Table 1. Partial sequencing of the *Ctrc* gene from genomic DNA of inbred mouse strains

Region	Variant	129S6	BALB/c	C3H	C57BL/6N	DBA/1	FVB
Intron 1	c.40+428T>C	+				+	
Intron 1	c.41-464C>A	+	+	+		+	
Intron 1	c.41-399G>C	+	+	+		+	
Intron 1	c.41-397C>T		+	+			
Intron 1	c.41-387T>C	+	+	+		+	
Intron 1	c.41-331T>C	+	+	+		+	
Intron 1	c.41-274C>A		+	+			
Intron 1	c.41-223T>C	+	+	+		+	
Intron 1	c.41-111T>C	+	+	+		+	
Intron 1	c.41-110_109delGT		+	+			
Intron 1	c.41-91A>C	+	+	+		+	
Intron 1	c.41-66G>A		+	+			
Intron 1	c.41-15T>C		+	+			
Exon 2	c.111C>T, p.Val37=		+	+			
Exon 2	**c.116_117insT**	+	+	+		+	+
Intron 2	c.131+12T>G		+	+			
Intron 2	c.132-41G>A					+	

See Methods for experimental details. The presence of the indicated variants is denoted by the + sign. All variants were homozygous. The c.116_117insT variant highlighted in bold indicates the absence of the c.117delT deletion in all strains but C57BL/6N. We also observed variations in the CA repeats within intron 1, c.41–157CA(23), but we did not determine the exact numbers. The C57BL/6J NC_000070.6 genomic sequence was used as reference.

C57BL/6J). This was further corroborated by PCR amplification and comparative DNA sequencing of exon 2 of *Ctrc* from C57BL/6N and FVB genomic DNA (data not shown). The c.117delT deletion causes a shift in the translational reading frame after Pro38 followed by a premature stop codon at position 80. Consequently, the mRNA likely undergoes nonsense-mediated decay, resulting in diminished levels of the full-length *Ctrc* mRNA, as evidenced by the RT-PCR data. Interestingly, however, skipping of exon 3 restores the reading frame and stabilizes the mRNA, which codes for a defective CTRC protein containing a large deletion (Supplemental Figure 1; supplemental material available online with this article; https://doi.org/10.1172/jci.insight.129717DS1). Although data are not shown, we tried to express this CTRC variant in HEK 293T cells but observed no secreted protein, suggesting intracellular retention and degradation. It remains unclear whether deletion c.117delT actually stimulates exon skipping or it just stabilizes a spurious splicing product that would be normally degraded. Taken together, the data indicate that the inbred mouse strain C57BL/6 is naturally deficient in CTRC because of a single-nucleotide deletion in the coding DNA.

Generation of the Ctrc$^+$ mouse strain on the C57BL/6N background. To evaluate the effect of CTRC deficiency on mouse physiology and pancreatitis responses, we generated a C57BL/6N strain with a functional *Ctrc* gene, as described in Methods. Briefly, we backcrossed the *Ctrc* locus from the inbred FVB strain onto the C57BL/6N background and designated the strain as *Ctrc*$^+$ (Supplemental Figure 2). We chose FVB as the donor strain for *Ctrc* because DNA sequencing of exons 2 and 3 and the flanking intronic regions from genomic DNA indicated complete identity of the locus with the exception of the c.117delT deletion in exon 2, while other inbred strains contained additional sequence variations (Table 1). RT-PCR and DNA sequencing of pancreatic cDNA from FVB mice showed a perfect match with the *Ctrc* mRNA reference sequence, while the other strains harbored various silent variants (data not shown). The *Ctrc*$^+$ strain was phenotypically unchanged relative to the parent C57BL/6N mice. All experiments described below were performed with homozygous *Ctrc*$^+$ mice.

Ctrc mRNA and CTRC protein expression studies. Analysis with semiquantitative RT-PCR and Western blot revealed that expression of *Ctrc* mRNA and CTRC protein was fully restored in *Ctrc*$^+$ mice (Figure 1, A and B). Total trypsinogen content in the pancreas of *Ctrc*$^+$ mice versus C57BL/6N controls was comparable, while chymotrypsinogen content was slightly elevated, although the difference was not statistically significant (Figure 2A). To obtain an estimate of the CTRC protein levels in the pancreas of *Ctrc*$^+$ mice, we performed Western blot analysis of pancreatic homogenates and compared the signal intensity to those of purified, recombinant mouse CTRC standards (Figure 2B). We found that CTRC protein content corresponded to

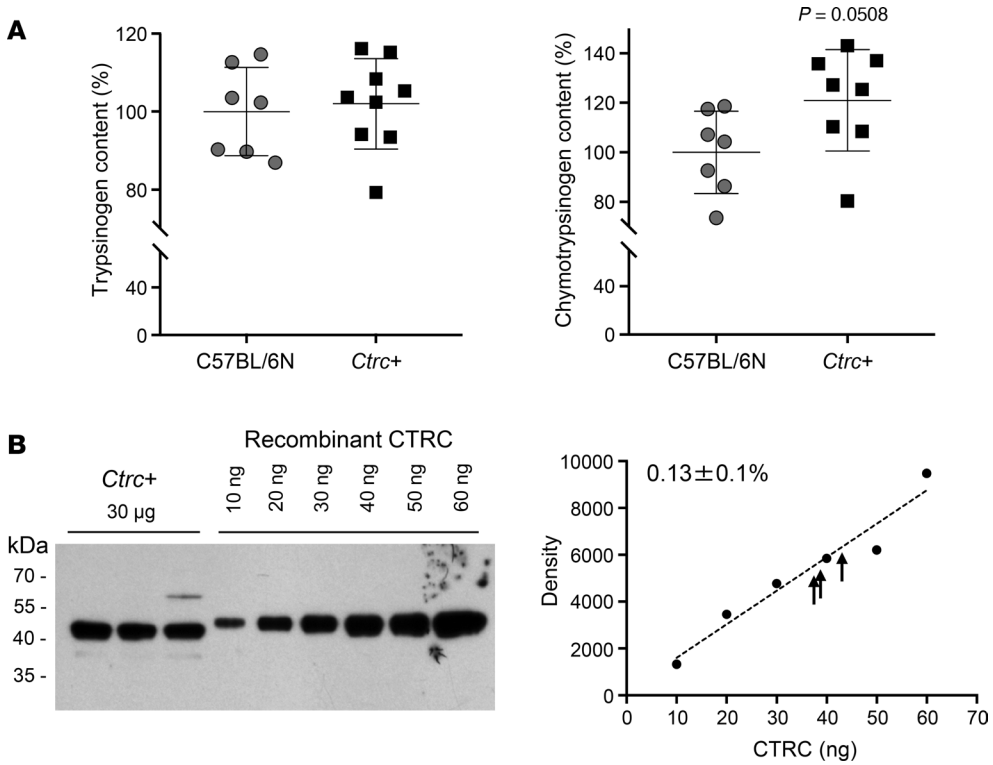

Figure 2. Protease zymogen levels in the pancreas of *Ctrc*⁺ mice. (**A**) Total trypsinogen and chymotrypsinogen content of pancreas homogenates (n = 7–9). Individual data points with mean and SD are shown. The difference of means was analyzed by 2-tailed, unpaired t test. (**B**) CTRC protein levels in the *Ctrc*⁺ mouse pancreas assessed by Western blotting. Samples of pancreatic homogenates loaded contained 30 µg total protein. Purified, His-tagged, recombinant mouse CTRC was used as calibration standards. Note the slightly higher migration due to the tag. The right side indicates the densitometry of the Western blot. The recombinant CTRC protein amount was plotted as a function of density. The arrows point to the density values of the *Ctrc*⁺ homogenates. The percentage value is the average CTRC content of mouse pancreas homogenates (mean ± SD). Representative gel and densitometry from 2 independent experiments are shown.

approximately 0.1% of the total protein content of pancreatic homogenates. The mouse *Ctrc* gene is located in the immediate vicinity of the *Cela2a* gene, encoding the digestive protease elastase 2A (CELA2A), which is flanked by the *Casp9* gene, encoding caspase-9. To rule out that expression of these protease genes was affected by the backcrossing, we performed Western blot analysis for the mouse CELA2A protein. Levels of CELA2A in pancreatic homogenates of *Ctrc*⁺ and C57BL/6N mice were similar (Supplemental Figure 3).

Acute pancreatitis in Ctrc⁺ *mice*. To study whether the restoration of a functional *Ctrc* gene in C57BL/6N mice had an effect on disease severity in experimentally induced acute pancreatitis, we challenged the mice with 12 hourly injections of cerulein and sacrificed them 1 hour after the last injection. Examination of H&E-stained pancreas sections of *Ctrc*⁺ mice revealed reduced edema, decreased inflammatory cell infiltration, and less acinar cell necrosis compared with C57BL/6N controls (Figure 3, A and B). Measurement of pancreatic water content confirmed the decreased edema in *Ctrc*⁺ mice relative to C57BL/6N, although the difference did not reach statistical significance (Figure 4A). Plasma amylase activity was significantly lower in cerulein-injected *Ctrc*⁺ mice compared with C57BL/6N controls (Figure 4B). Similarly, significantly reduced tissue myeloperoxidase (MPO) content was found in the pancreas of cerulein-treated *Ctrc*⁺ mice relative to the C57BL/6N controls (Figure 4C), indicating decreased neutrophil sequestration. Taken together, these observations clearly demonstrate that cerulein-induced acute pancreatitis was less severe in *Ctrc*⁺ mice than in C57BL/6N animals.

Chronic pancreatitis in Ctrc⁺ *mice*. To assess whether repeated acute insults would result in different levels of chronic damage in *Ctrc*⁺ and C57BL/6N mice, we induced chronic pancreatitis by a 10-week cerulein injection protocol, as described in Methods. H&E-stained pancreas sections of cerulein-treated animals showed abnormal tissue architecture with acinar cell atrophy and pseudotubular complexes. All these pathological features of chronic pancreatitis were significantly milder in *Ctrc*⁺ mice compared with

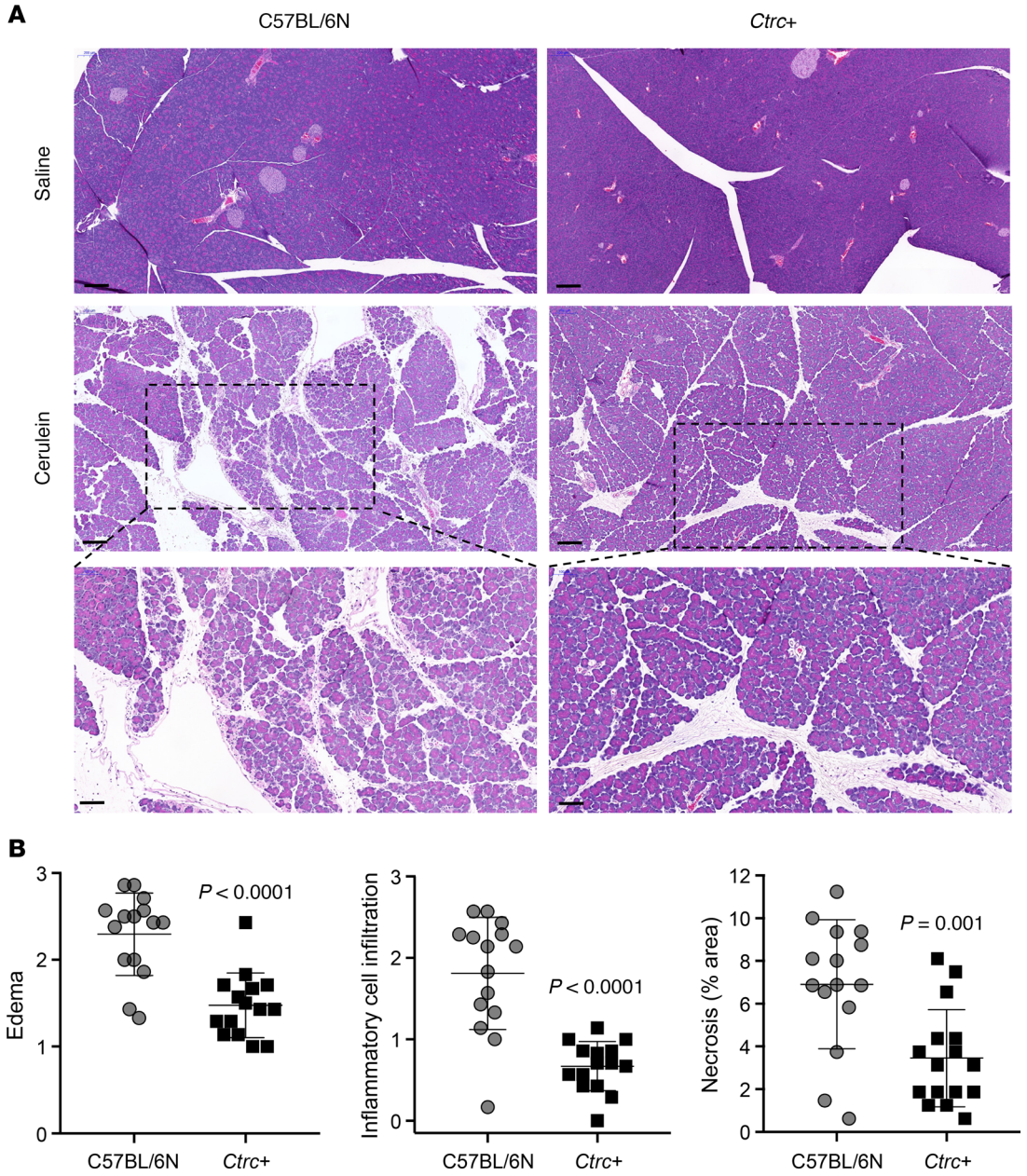

Figure 3. Cerulein-induced acute pancreatitis in *Ctrc*$^+$ mice. (**A**) Representative H&E-stained histological sections of the pancreas from mice given saline (n = 10) or cerulein (n = 15). Scale bars: 200 μm (top and middle), 100 μm (bottom). (**B**) Histology scoring of H&E-stained pancreas sections for edema, inflammatory cell infiltration, and acinar cell necrosis in cerulein-treated mice (n = 15). Individual data points with mean and SD are shown. Differences of means were analyzed by 2-tailed, unpaired t test. See Methods for details.

C57BL/6N controls (Figure 5, A and B). Loss of parenchyma was also evidenced by the reduced weight of the pancreas. Cerulein-treated *Ctrc*$^+$ animals showed higher pancreas weight than C57BL/6N mice (Figure 6A), indicating less atrophy, which was in agreement with the histological findings. Fibrosis was also less apparent in *Ctrc*$^+$ mice versus C57BL/6N controls, as judged by the hydroxyproline content of the pancreas (Figure 6B) and Masson's trichrome staining (Figure 7). We conclude that severity of chronic pancreatitis was improved in *Ctrc*$^+$ mice.

Intrapancreatic trypsin activity in Ctrc$^+$ *mice*. The most straightforward explanation for the protective effect of CTRC against acute and chronic pancreatitis is that CTRC-mediated trypsinogen degradation mitigates cerulein-induced intra-acinar trypsin activation. To test this notion, we determined trypsin and chymotrypsin activities in pancreas homogenates of *Ctrc*$^+$ and C57BL/6N mice. Protease activities were assessed at

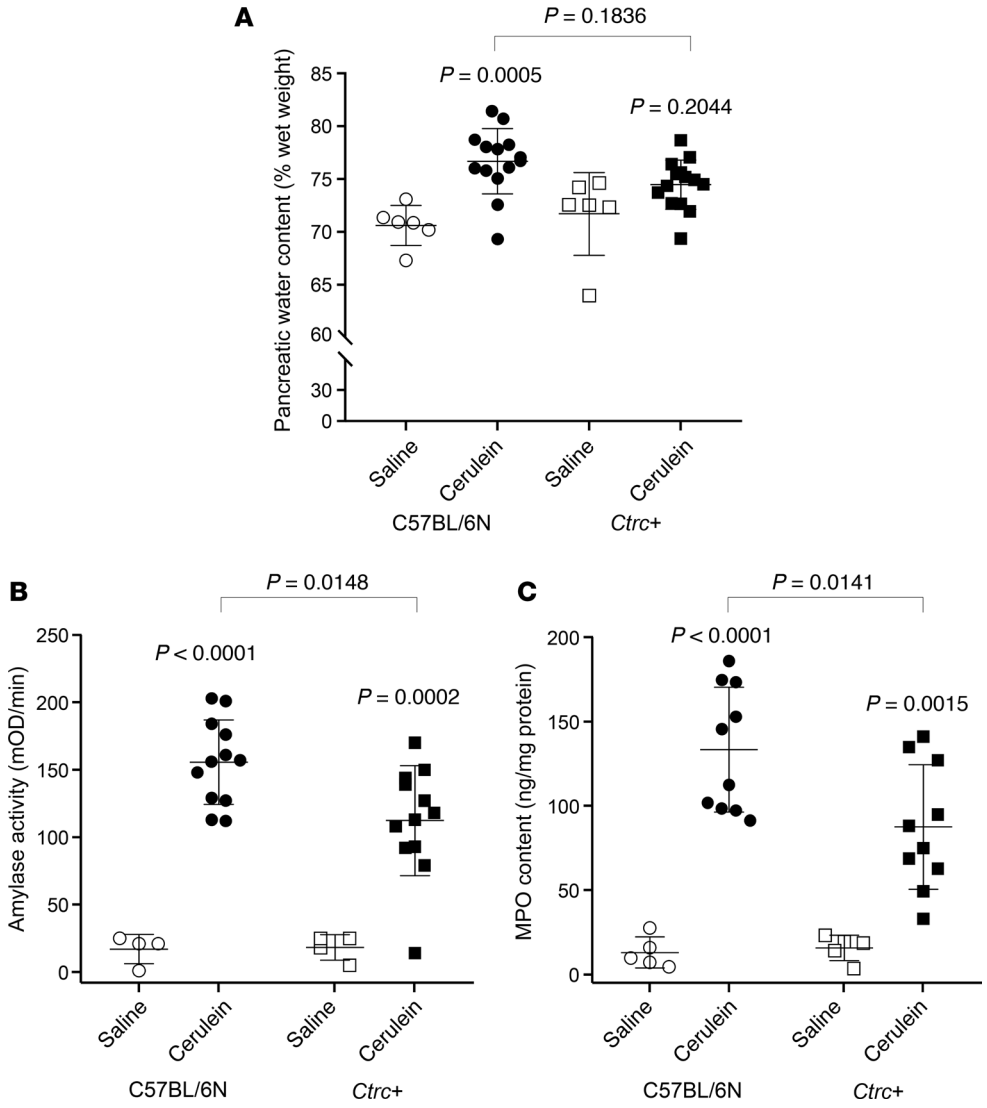

Figure 4. Pancreas edema, plasma amylase activity, and pancreas MPO content in *Ctrc*$^+$ mice with acute pancreatitis. (**A**) Pancreatic water content of C57BL/6N and *Ctrc*$^+$ mice treated with saline (n = 6) or cerulein (n = 14). (**B**) Plasma amylase activity in C57BL/6N and *Ctrc*$^+$ mice treated with saline (n = 4) or cerulein (n = 12). (**C**) Pancreatic MPO content of C57BL/6N and *Ctrc*$^+$ mice treated with saline (n = 5) or cerulein (n = 10). Individual data points with mean and SD are shown. Statistical comparison of means was performed by 1-way ANOVA and Tukey's post hoc test. See Methods for experimental details.

30 minutes after a single cerulein injection to avoid interference by inflammatory cells. As predicted, significantly decreased trypsin activity was seen in the pancreas of *Ctrc*$^+$ mice relative to C57BL/6N controls (Figure 8A). Chymotrypsin activity in *Ctrc*$^+$ mice, however, showed only a slight but not significant decrease (Figure 8B), which may be related to the higher chymotrypsinogen content of this strain. These observations indicate that restoration of a functional *Ctrc* gene in C57BL/6N mice mitigated intrapancreatic trypsin activation and reduced the severity of cerulein-induced pancreatitis.

Discussion

Chymotrypsins are powerful digestive proteases that are produced in multiple isoforms by the pancreas. Remarkably, they play a protective role against pancreatitis by controlling harmful trypsin levels through degradation of trypsinogens (2). In humans, the primary regulator of trypsinogen activation is the minor isoform CTRC, while the highly abundant CTRB1 and CTRB2 isoforms contribute much less to trypsinogen degradation (8). Our recent study demonstrated that in mice the major chymotrypsin isoform CTRB1 (mice have no CTRB2 gene) plays a more significant role in protection against pancreatitis and deletion

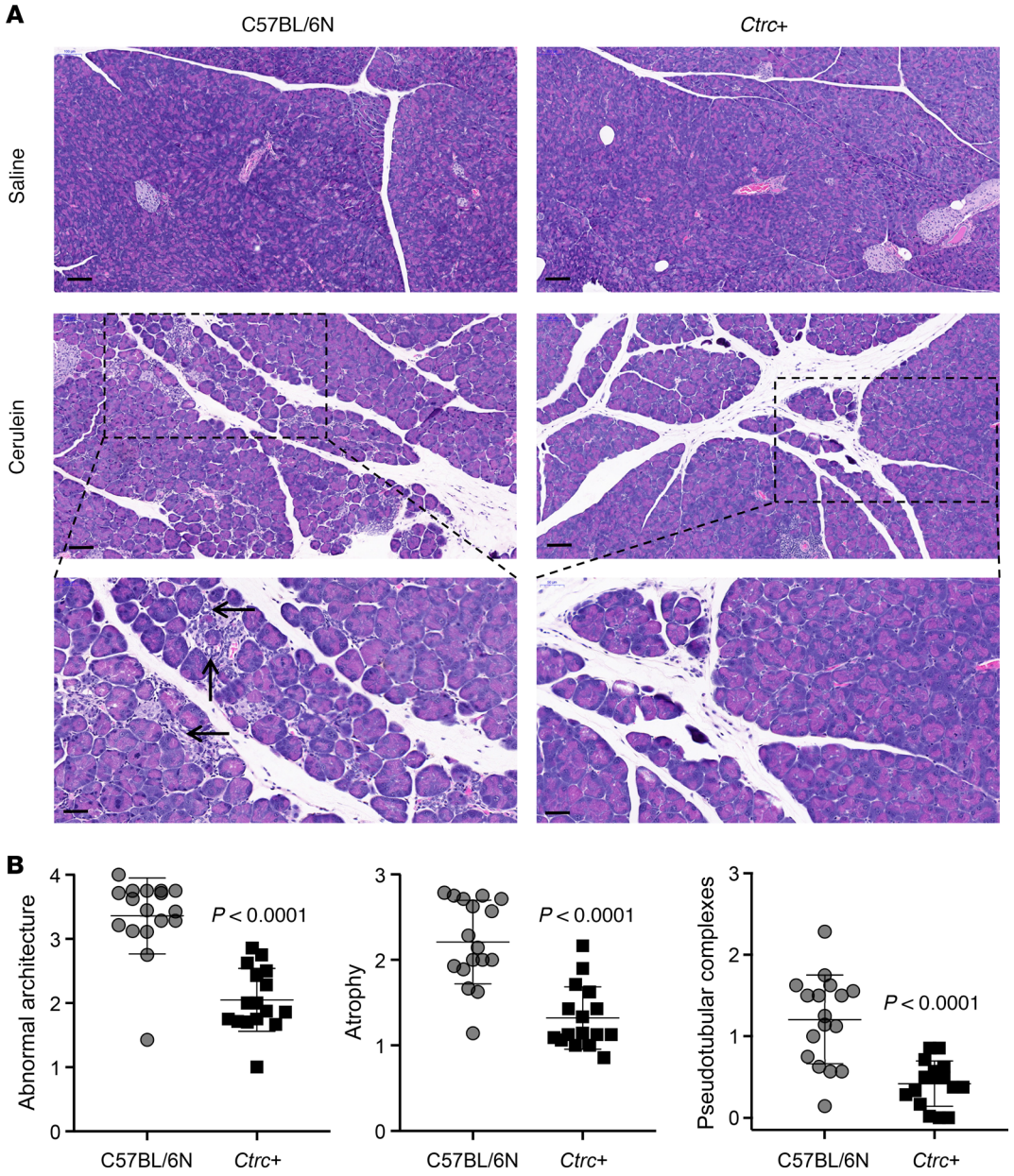

Figure 5. Cerulein-induced chronic pancreatitis in *Ctrc*⁺ mice. (**A**) Representative H&E-stained histological sections of the pancreas from mice given saline (n = 6–8) or cerulein (n = 16–17). Scale bars: 100 μm (top and middle), 50 μm (bottom). Arrows point to pseudotubular complexes. (**B**) Histology scoring of H&E-stained pancreas sections for abnormal tissue architecture, acinar cell atrophy, and pseudotubular complexes in cerulein-treated mice (n = 16–17). Individual data points with mean and SD are shown. Differences of means were analyzed by 2-tailed, unpaired t test. See Methods for details.

of this isoform results in severer cerulein-induced pancreatitis (9). In the present study, we set out to characterize the role of mouse CTRC in pancreatitis. Even though human genetic and biochemical studies strongly implicate CTRC as a susceptibility gene for pancreatitis, animal model evidence to support this notion has been lacking. Surprisingly, we found that C57BL/6 mice (both the J and N substrains) are naturally deficient in CTRC because of a single-nucleotide deletion in exon 2 of the *Ctrc* gene. We restored a functional *Ctrc* locus in C57BL/6N mice (*Ctrc*⁺ strain) by backcrossing with FVB mice for several generations. To assess whether *Ctrc*⁺ mice are better protected against pancreatitis, we compared cerulein-induced acute and chronic pancreatitis between the *Ctrc*⁺ and C57BL/6N strains. Our results demonstrated that pancreatitis severity was ameliorated in *Ctrc*⁺ mice relative to the C57BL/6N controls in both the acute and chronic disease models. Importantly, cerulein-induced trypsin activation was reduced in *Ctrc*⁺ mice, consistent with the proposed mechanistic link between CTRC-mediated trypsinogen degradation

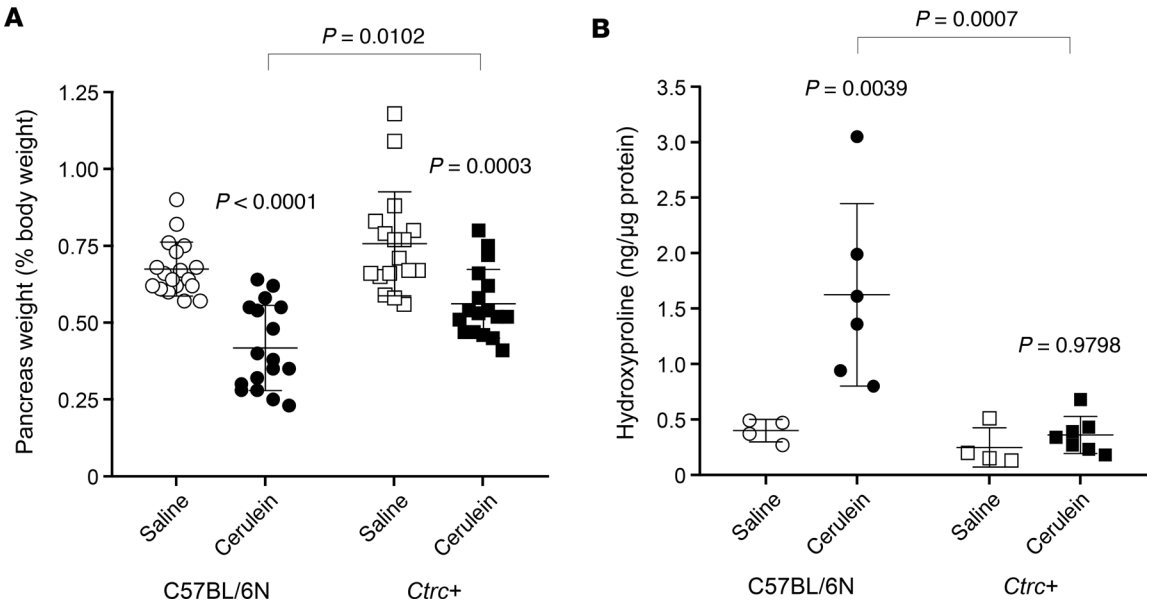

Figure 6. Pancreas atrophy and hydroxyproline content in *Ctrc*⁺ mice with chronic pancreatitis. (**A**) Pancreas weight of C57BL/6N and *Ctrc*⁺ mice given saline (n = 17–18) or cerulein (n = 17), expressed as percentage of the body weight. (**B**) Hydroxyproline content of the pancreas of C57BL/6N and *Ctrc*⁺ mice given saline (n = 4) or cerulein (n = 6–7). Individual data points with mean and SD are shown. Statistical comparison of means was performed by 1-way ANOVA and Tukey's post hoc test. See Methods for technical details.

and less severe pancreatitis. Taken together, these experiments demonstrated the protective role of CTRC against pancreatitis in rodents and identified the C57BL/6 mice as a natural model for loss-of-function CTRC mutations in humans.

The observations also provide support for the long-held contention that intrapancreatic trypsin activation in cerulein-induced pancreatitis is a pathogenic driver (11, 12). However, other studies called into question the central role of trypsin in cerulein-induced pancreatitis. Genetic deletion of mouse cationic trypsinogen (isoform T7) resulted in diminished intrapancreatic trypsin activation, yet cerulein-induced acute pancreatitis was only slightly affected and chronic pancreatitis was unchanged (13, 14). Similarly, global deletion of cathepsin B, the lysosomal enzyme initiating intra-acinar trypsinogen activation, abolished trypsin activation yet caused only a modest decrease in the severity of pancreatitis (15). Finally, Van Acker et al. found that intrapancreatic trypsin activation is responsible only for increased organelle fragility during cerulein-induced pancreatitis while other early events, such as colocalization of zymogen granules and lysosomes, were mediated by trypsin-independent pathways (16). Our studies with the CTRB1-deficient mouse model (*Ctrb1-del* mice), on the other hand, demonstrated that increased intrapancreatic trypsin activation is paralleled by severer pancreatitis (9). More recently, transgenic mice carrying a furin-activated trypsinogen construct were shown to exhibit severer pancreatitis responses when challenged with cerulein (17). The reason for the discrepancy in the results among the various studies is not readily apparent; however, one must keep in mind that all models have limitations, which warrant caution when it comes to interpretation. Thus, when T7 was deleted, at least 3 other abundantly expressed trypsinogen isoforms were still present in the mouse pancreas (10). Global deletion of cathepsin B can have multiple other effects that may alter pancreatitis severity, e.g., through affecting immune cells. The transgenic mice with furin-sensitive trypsinogen were crossed with a Cre driver, which is an additional confounding factor. Finally, our *Ctrc*⁺ strain contains not only a functional *Ctrc* gene transferred from FVB mice but also the adjacent chromosomal regions, which may influence pancreatitis responses. We are also mindful that cerulein activates other signaling pathways and may cause endoplasmic reticulum stress and metabolic changes, which can drive the inflammatory process independently of trypsin (18).

In contrast with the brewing controversy regarding the role of trypsin in rodent models of secretagogue-induced pancreatitis, there is agreement that increased intrapancreatic trypsin activity causes pancreatitis in humans. The trypsin-dependent pathway in chronic pancreatitis is associated with mutations in the high-impact genes *PRSS1*, *SPINK1*, and *CTRC* (2). In addition, other genetic variations within this

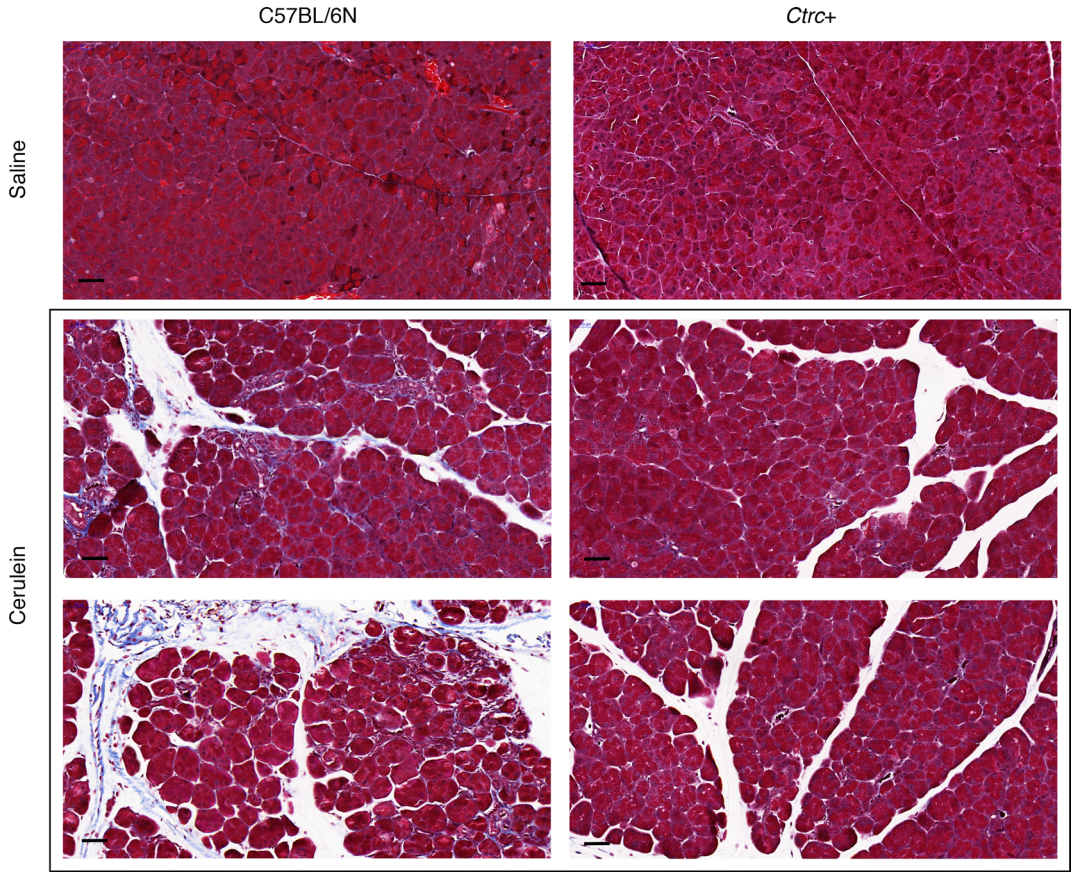

Figure 7. Pancreas fibrosis in *Ctrc*$^+$ mice with chronic pancreatitis. Masson's trichrome staining highlights collagen in blue. Representative histological sections of the pancreas from mice given saline (n = 6–8) or cerulein (n = 16–17) are shown. Scale bars: 50 μm.

pathway have lower impact protective effects, such as the p.G191R variant in *PRSS2*, a protective haplotype in the *PRSS1-PRSS2* locus, and the inversion at the *CTRB1-CTRB2* locus. All genetic changes ultimately affect the rate and extent of autoactivation of trypsinogen to trypsin. We recently succeeded in modeling the pathogenic effect of a rapidly autoactivating trypsinogen mutant in mice (19). In the *T7D23A* mouse strain the mouse cationic trypsinogen gene carries the heterozygous p.D23A mutation, which markedly stimulates autoactivation. Remarkably, *T7D23A* mice develop spontaneous acute pancreatitis at an early age, which progresses to chronic pancreatitis.

It is important to note, however, that not all forms of human pancreatitis are trypsin dependent. Thus, pancreatitis associated with biliary disease, hypertriglyceridemia, endoscopic retrograde cholangiopancreatography, trauma, or infection is triggered by other causes. A subset of genetically determined pancreatitis cases is caused by mutation-induced misfolding and resultant endoplasmic stress (20, 21). These types of pancreatitis are not associated with loss-of-function *CTRC* mutations. Alcoholic pancreatitis, on the other hand, develops via a trypsin-mediated mechanism where genetic and environmental factors synergize and CTRC mutations frequently contribute to disease onset (8). Overall, chymotrypsin-dependent trypsinogen degradation exerts its protective effect only in the setting of pathological intrapancreatic trypsin activation caused by genetic mutations in humans or by experimental cerulein stimulation in mice.

Multiple reports described that various mouse strains respond differently when pancreatitis is elicited by repeated cerulein injections (22–25). The genetic factors underlying these phenotypic differences have not been clarified, and this represents an opportunity to unveil determinants of disease onset and severity. In this respect, *Ctrc* is the first gene to our knowledge that has been convincingly demonstrated to cause strain-specific differences in pancreatitis in mice. Furthermore, the *Ctrc*$^+$ strain, with the congenic C57BL/6N mice, can serve as a valuable preclinical tool for testing pharmacological interventions designed to modify CTRC function.

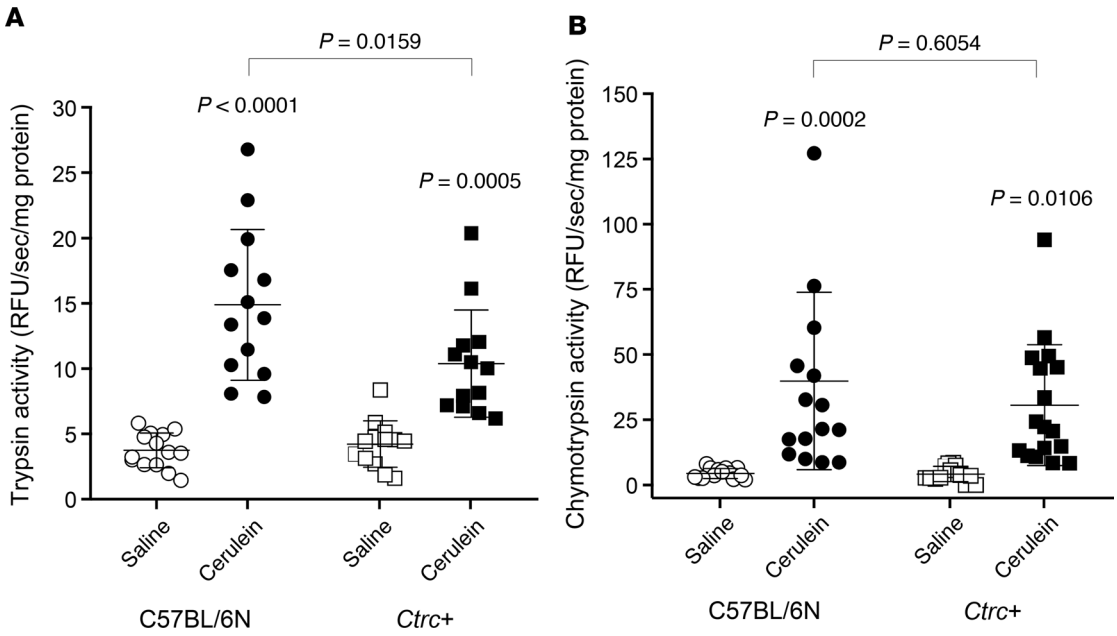

Figure 8. Intrapancreatic protease activation in Ctrc+ mice. Trypsin (**A**) and chymotrypsin (**B**) activities were determined 30 minutes after a single saline (n = 13–14) or cerulein (n = 13–17) injection. Individual data points with mean and SD are shown. Statistical comparison of means was performed by 1-way ANOVA and Tukey's post hoc test. See Methods for assay description.

Methods

Accession numbers and nomenclature. As genomic reference sequence, we used NC_000070.6, *Mus musculus* strain C57BL/6J chromosome 4, GRCm38.p4 C57BL/6J. This sequence contains the c.117delT single-nucleotide deletion in exon 2 of the *Ctrc* gene. As the *Ctrc* coding reference sequence, we used NM_001033875.2, *Mus musculus* chymotrypsin C (caldecrin) (Ctrc), transcript variant 1, mRNA. This sequence was derived from pancreatic cDNA clones of an unspecified mouse strain and codes for a functional CTRC protein. The sequence is identical with that predicted from the C57BL/6J genomic reference, with the exception of the c.117delT deletion. Nucleotide numbering of the coding DNA starts with the first nucleotide of the translation initiation ATG codon.

Mouse CTRC protein. Recombinant mouse CTRC with a C-terminal 10His tag was expressed in HEK 293T cells and purified as described previously (10).

Animals. Inbred male mice 129S6 (129S6/SvEvTac), BALB/c (BALB/cAnNTac), C3H (C3H/HeNTac), DBA/1 (DBA/1JBomTac), and FVB (FVB/NTac) were obtained from Taconic Biosciences. C57BL/6J and C57BL/6N mice were purchased from Charles River Laboratories. C57BL/6N mice were also produced in our breeding facility from the same stock. The *Ctrc*$^+$ strain was generated as described below. The number of animals used in each experiment is shown in the figures. This represents a pooled value from 2 or 3 independent experiments using 5–9 animals in the cerulein-treated groups and 2–4 mice in the saline-treated groups. Experimental numbers for the different severity indicators may vary because not all mice were analyzed for all parameters. Both males and females were studied. Experimental mice were 10–12 weeks old and weighed around 25 g (males) and 20 g (females).

Generation of the Ctrc$^+$ *mouse strain*. We backcrossed the *Ctrc* locus from the inbred FVB strain onto the C57BL/6N background using marker-assisted accelerated backcrossing (MaxBax, Charles River Laboratories; Supplemental Figure 2). During this process, we genotyped the offspring using a mouse 384 single nucleotide polymorphism (SNP) panel and then selectively bred mice, which had a normal *Ctrc* locus and contained most of the C57BL/6N genome. The 384 SNP panel uses evenly spaced polymorphic markers covering the entire mouse genome with about half of the SNPs being polymorphic between the 2 strains crossed. After 8 generations of backcrossing, we successfully restored the *Ctrc* gene in the C57BL/6N mouse. The final strain, which showed a 100% SNP match with the C57BL/6N background, was designated as *Ctrc*$^+$. The *Ctrc*$^+$ strain was bred to homozygosity and maintained in the homozygous state. The strain showed no morphological or behavioral differences from the parent C57BL/6N mice.

Genotyping. To genotype *Ctrc*$^{+}$ mice, we used primers that amplified a 530-nt genomic sequence (529 nt in C57BL/6) that included exons 2 and 3 of the *Ctrc* gene with the flanking intronic sequences from c.41-183 to c.230+74 (c.229+74 in C57BL/6). The absence of the c.117delT deletion was then verified by DNA sequencing. The primer sequences were as follows: forward primer 5′-CCTGATTGAGGTCATTCTTCC-3′, reverse primer 5′-AGGACAGCAGCTAACAGAG-3′.

Genomic sequencing of mouse Ctrc. Exons 2 and 3 with intervening intron 2 and flanking intron 1 and intron 3 sequences were sequenced after PCR amplification from genomic DNA with the following primers: forward primer 5′-TGACCGGTGTTTGGTTTG-3′, reverse primer 5′-CCGAGAAGCGATATGTCAAC-3′. The amplicon was 1014 nt (1013 nt in C57BL/6) and included sequences from c.40+337 to c.230+121 (c.229+121 in C57BL/6).

Histological analysis. Pancreas tissue was fixed in 10% neutral buffered formalin, parafin-embedded, sectioned, and stained with H&E or Masson's trichrome staining at the Boston University Experimental Pathology Laboratory Service Core. Severity of acute and chronic pancreatitis was graded blinded to experimental condition using an arbitrary semiquantitative scoring system. At least 10 randomly selected visual fields per slide were scored and averaged. For acute pancreatitis, the extent of edema and the presence of inflammatory cells were scored as follows: 0 = absent, 1 = mild (<10% of visual field), 2 = moderate (10%–50%), and 3 = severe (>50%). Acinar cell necrosis was estimated by visual inspection and expressed as percentage of tissue area. For chronic pancreatitis, areas of abnormal pancreatic tissue architecture were scored as follows: 0 = absent, 1 = rare, 2 = mild (<10% of visual field), 3 = moderate (10%–50%), and 4 = severe (>50%). Within these areas, acinar cell atrophy and the presence of pseudotubular complexes were scored as follows: 0 = absent, 1 = mild (<10% of visual field), 2 = moderate (10%–50%), and 3 = severe (>50%).

RT-PCR of mouse Ctrc. Total RNA was extracted from mouse pancreas tissue (~30 mg) using the RNeasy Plus Mini Kit (Qiagen). RNA (2 μg) was reverse-transcribed with the High Capacity cDNA Reverse Transcription Kit (4368814, Thermo Fisher Scientific). Using pancreatic cDNA as template, a 717-nt segment between c.8 and c.724 of the 804-nt-long *Ctrc* coding DNA was PCR amplified with the following primers: forward primer 5′-GAATTACAGTCCTCGCTGC-3′, reverse primer 5′-CTCTACTGGAACCAAAGCTC-3′. The PCR products were analyzed by agarose gel electrophoresis with ethidium bromide staining and by direct DNA sequencing. As loading control, 18S rRNA was amplified, as described previously (9). The 1 Kb Plus DNA ladder (10787018, Thermo Fisher Scientific) was used as markers for agarose gel electrophoresis.

Western blotting. For Western blotting, mouse pancreas tissue was homogenized in ice-cold PBS supplemented with protease inhibitors, and aliquots of 2.5 μg to 30 μg total protein, as indicated, were electrophoresed on 15% SDS-PAGE minigels (made in-house) and transferred onto an Immobilon-P membrane (MilliporeSigma). After blocking with 5% nonfat milk in PBS supplemented with 0.1% Tween-20, the membrane was incubated with the primary and secondary antibodies for 1 hour each at room temperature. The bands were detected using SuperSignal West Pico Chemiluminescent Substrate (Thermo Fisher Scientific). Antibodies and dilutions used in this study were as follows. A sheep polyclonal antibody against human CTRC was used at 1:500 dilution (AF6907, R&D Systems). A rabbit polyclonal antibody against mouse CELA2A was used at 1:5000 dilution (A54384, EpiGentek). A rabbit monoclonal antibody against ERK1/2 was used at 1:500 dilution (137F5, Cell Signaling Technology). As secondary antibodies, HRP-conjugated donkey anti-sheep IgG was used at 1:4000 dilution (HAF016, R&D Systems), and HRP-conjugated goat anti–rabbit IgG was used at 1:5000 dilution (31460, Thermo Fisher Scientific).

Protease zymogen content in pancreas homogenates. Trypsinogen and chymotrypsinogen levels in the pancreas were characterized by measuring enzymatic activity after maximal activation, as described recently (19). Briefly, pancreas (40 mg) was homogenized in 400 μL 20-mM Na-HEPES (pH 7.4), and the homogenate was cleared by centrifugation (1000 *g*, 10 minutes, 4°C). To activate trypsinogen, an aliquot (5 μL) of the supernatant was treated with 4 μL human enteropeptidase (50× dilution of 1585-SE, R&D Systems) in 100 μL final volume of 0.1 M Tris-HCl (pH 8.0), 10 mM $CaCl_2$, and 0.05% Tween-20. The endogenous active trypsin served as the activator for chymotrypsinogen. The development of trypsin and chymotrypsin activity was followed every 5 minutes by withdrawing a 2-μL aliquot and mixing it with 48 μL assay buffer (0.1 M Tris-HCl at pH 8.0, 1 mM $CaCl_2$, 0.05% Tween-20) and 150 μL *N*-CBZ-Gly-Pro-Arg-pNA or Suc-Ala-Ala-Pro-Phe-pNA substrate (Bachem USA) dissolved in assay buffer. The increase

in absorbance was monitored in a Spectramax Plus 384 microplate reader (Molecular Devices) at 405 nm, and the rate of substrate cleavage was normalized to the total protein concentration and expressed as percentage of the C57BL/6N control value.

Cerulein-induced acute pancreatitis. Acute pancreatitis was induced by repeated intraperitoneal injections of the secretagogue peptide cerulein in a supramaximal stimulatory dose. Twelve hourly injections of cerulein (C9026, MilliporeSigma) dissolved in normal saline (10 μg/mL) were administered intraperitoneally at a dose of 50 μg/kg. Experimental control mice were given normal saline injections. Mice were sacrificed 1 hour after the 12th injection, and the pancreas and blood were harvested. For histological analysis, pancreas tissue was fixed in 10% neutral buffered formalin. For MPO assays, a portion of the pancreas was snap-frozen in liquid nitrogen and stored at –80°C until use. Blood was drawn by cardiac puncture into heparinized syringes and centrifuged at 2000 *g* for 10 minutes at 4°C to obtain plasma, which was stored at –80°C until use.

Determination of pancreatic water content. To characterize tissue edema, approximately 50 mg of the pancreas was weighed, dried for 72 hours in an oven at 65°C, and weighed again. Tissue water content was then expressed as percentage of the wet weight.

Plasma amylase activity. Levels of amylase in the blood were determined enzymatically using the substrate 2-chloro-*p*-nitrophenyl-α-D-maltotrioside (A7564-60, Pointe Scientific). Plasma (1 μL) was diluted with 9 μL normal saline and mixed with 190 μL substrate to start the reaction. The increase in absorbance due to the release of 2-chloro-*p*-nitrophenol was monitored in a microplate reader at 405 nm for 2 minutes. The rate of substrate cleavage was expressed in mOD/min units.

Pancreatic MPO content. Pancreatic tissue levels of MPO were determined using an ELISA kit (HK210-01, Hycult Biotech) according to the manufacturer's instructions. The ELISA signal measured at 450 nm was converted to nanogram per milliliter MPO concentration using a calibration curve, normalized to total protein concentration (0.4 mg/mL in the 100-μL reaction sample), and expressed as nanogram MPO per milligram protein.

Cerulein-induced chronic pancreatitis. Chronic pancreatitis was elicited by a repeated series of intraperitoneal cerulein injections (50 μg/kg body weight dose per injection). Mice were given 6 hourly injections of cerulein on Mondays and Thursdays for 10 weeks. Animals were sacrificed 8 days after the last injection and pancreata were harvested. Control animals received normal saline injections.

Tissue hydroxyproline determination. Pancreatic hydroxyproline content was determined as described previously (21). Briefly, the reaction of oxidized hydroxyproline with 4-(dimethylamino)benzaldehyde (MAK008, MilliporeSigma) was measured. Values were normalized to total protein and expressed in nanograms of hydroxyproline per microgram of protein units.

Intrapancreatic trypsin and chymotrypsin activation. Cerulein-induced intra-acinar protease activation was determined at 30 minutes after a single cerulein injection (50 μg/kg body weight dose), as described previously (9), with the exception that the Z-Gly-Pro-Arg-AMC fluorescent substrate (Bachem USA) was used for trypsin activity determination. The rate of substrate cleavage was normalized to the total protein in the assay mixture, and enzyme activity was expressed as relative fluorescent units per second per milligram protein.

Statistics. Results were plotted as individual data points with the mean and SD indicated. Differences of means between 2 groups were analyzed by 2-tailed, unpaired *t* test. For multiple groups, statistical comparison of means was performed by 1-way ANOVA and Tukey's post hoc test. $P < 0.05$ was considered statistically significant.

Study approval. All animal experiments were performed at Boston University. We have complied with all relevant ethical regulations. Animal experiments were performed with the approval and oversight of the Institutional Animal Care and Use Committee of Boston University, including protocol review and after approval monitoring. The animal care program at Boston University is managed in full compliance with the US Animal Welfare Act, the US Department of Agriculture Animal Welfare Regulations, the US Public Health Service Policy on Humane Care and Use of Laboratory Animals, and the National Research Council's *Guide for the Care and Use of Laboratory Animals* (National Academies Press). Boston University has an approved Animal Welfare Assurance statement (A3316-01) on file with the US Public Health Service, NIH, Office of Laboratory Animal Welfare, and has been accredited by the Association for Assessment and Accreditation of Laboratory Animal Care International.

Author contributions

MST conceived and directed the study. MST, AG, ZJ, and BCN designed the experiments. AG, ZJ, BCN, and EH performed the experiments. MST, AG, ZJ, and BCN analyzed the data. MST and AG wrote the manuscript, AG prepared the figures, and all authors contributed to revisions and approved the final version.

Acknowledgments

This work was supported by NIH grants R01 DK082412, R01 DK058088, and R01 DK117809 (to MST). EH and ZJ were also supported by research grants from the National Pancreas Foundation. All experiments were performed at Boston University.

Address correspondence to: Miklós Sahin-Tóth, 675 Charles East Young Drive South, MacDonald Research Laboratories, Room 2220, Los Angeles, California 90095, USA. Phone: 310.267.5905; Email: msahintoth@mednet.ucla.edu.

1. Yadav D, Lowenfels AB. The epidemiology of pancreatitis and pancreatic cancer. *Gastroenterology*. 2013;144(6):1252–1261.
2. Hegyi E, Sahin-Tóth M. Genetic risk in chronic pancreatitis: the trypsin-dependent pathway. *Dig Dis Sci*. 2017;62(7):1692–1701.
3. Szmola R, Sahin-Tóth M. Chymotrypsin C (caldecrin) promotes degradation of human cationic trypsin: identity with Rinderknecht's enzyme Y. *Proc Natl Acad Sci U S A*. 2007;104(27):11227–11232.
4. Szabó A, Sahin-Tóth M. Increased activation of hereditary pancreatitis-associated human cationic trypsinogen mutants in presence of chymotrypsin C. *J Biol Chem*. 2012;287(24):20701–20710.
5. Nemoda Z, Sahin-Tóth M. Chymotrypsin C (caldecrin) stimulates autoactivation of human cationic trypsinogen. *J Biol Chem*. 2006;281(17):11879–11886.
6. Jancsó Z, Sahin-Tóth M. Tighter control by chymotrypsin C (CTRC) explains lack of association between human anionic trypsinogen and hereditary pancreatitis. *J Biol Chem*. 2016;291(25):12897–12905.
7. Németh BC, Szücs Á, Hegyi P, Sahin-Tóth M. Novel PRSS1 mutation p.P17T validates pathogenic relevance of CTRC-mediated processing of the trypsinogen activation peptide in chronic pancreatitis. *Am J Gastroenterol*. 2017;112(12):1896–1898.
8. Rosendahl J, et al. Genome-wide association study identifies inversion in the *CTRB1-CTRB2* locus to modify risk for alcoholic and non-alcoholic chronic pancreatitis. *Gut*. 2018;67(10):1855–1863.
9. Jancsó Z, Hegyi E, Sahin-Tóth M. Chymotrypsin reduces the severity of secretagogue-induced pancreatitis in mice. *Gastroenterology*. 2018;155(4):1017–1021.
10. Németh BC, Wartmann T, Halangk W, Sahin-Tóth M. Autoactivation of mouse trypsinogens is regulated by chymotrypsin C via cleavage of the autolysis loop. *J Biol Chem*. 2013;288(33):24049–24062.
11. Lerch MM, Gorelick FS. Early trypsinogen activation in acute pancreatitis. *Med Clin North Am*. 2000;84(3):549–563.
12. Saluja AK, Lerch MM, Phillips PA, Dudeja V. Why does pancreatic overstimulation cause pancreatitis? *Annu Rev Physiol*. 2007;69:249–269.
13. Dawra R, et al. Intra-acinar trypsinogen activation mediates early stages of pancreatic injury but not inflammation in mice with acute pancreatitis. *Gastroenterology*. 2011;141(6):2210–2217.e2.
14. Sah RP, Dudeja V, Dawra RK, Saluja AK. Cerulein-induced chronic pancreatitis does not require intra-acinar activation of trypsinogen in mice. *Gastroenterology*. 2013;144(5):1076–1085.e2.
15. Halangk W, et al. Role of cathepsin B in intracellular trypsinogen activation and the onset of acute pancreatitis. *J Clin Invest*. 2000;106(6):773–781.
16. Van Acker GJ, Weiss E, Steer ML, Perides G. Cause-effect relationships between zymogen activation and other early events in secretagogue-induced acute pancreatitis. *Am J Physiol Gastrointest Liver Physiol*. 2007;292(6):G1738–G1746.
17. Zhan X, et al. Elevated intracellular trypsin exacerbates acute pancreatitis and chronic pancreatitis in mice. *Am J Physiol Gastrointest Liver Physiol*. 2019;316(6):G816-G825.
18. Whitehead RH, Robinson PS, Williams JA, Bie W, Tyner AL, Franklin JL. Conditionally immortalized colonic epithelial cell line from a Ptk6 null mouse that polarizes and differentiates in vitro. *J Gastroenterol Hepatol*. 2008;23(7 pt 1):1119–1124.
19. Geisz A, Sahin-Tóth M. A preclinical model of chronic pancreatitis driven by trypsinogen autoactivation. *Nat Commun*. 2018;9(1):5033.
20. Fu TY, Lou WY, Shi TL. [Variation feature of receptor binding sites of H1N1 influenza hemagglutinin in different hosts]. *Yi Chuan*. 2010;32(7):701–711.
21. Hegyi E, Sahin-Tóth M. Human *CPA1* mutation causes digestive enzyme misfolding and chronic pancreatitis in mice. *Gut*. 2019;68(2):301–312.
22. Wang J, et al. Relationship of strain-dependent susceptibility to experimentally induced acute pancreatitis with regulation of Prss1 and Spink3 expression. *Lab Invest*. 2010;90(5):654–664.
23. Ulmasov B, et al. CLIC1 null mice demonstrate a role for CLIC1 in macrophage superoxide production and tissue injury. *Physiol Rep*. 2017;5(5):e13169.
24. Stumpf F, et al. Metamizol relieves pain without interfering with cerulein-induced acute pancreatitis in mice. *Pancreas*. 2016;45(4):572–578.
25. Iyer S, et al. Clusterin and Pycr1 alterations associate with strain and model differences in susceptibility to experimental pancreatitis. *Biochem Biophys Res Commun*. 2017;482(4):1346–1352.